

Title	Functionalization of germanium nanowires
Authors	Collins, Gillian;Fleming, Peter G.;O'Dwyer, Colm;Morris, Michael A.;Holmes, Justin D.
Publication date	2011-01
Original Citation	Collins, G., Fleming, P., O'Dwyer, C., Morris, M. A., and Holmes, J. D. (2011) 'Functionalization of Germanium Nanowires', ECS Transactions, 35(8), pp. 89-99; doi:10.1149/1.3567740
Type of publication	Article (peer-reviewed)
Link to publisher's version	http://ecst.ecsdl.org/content/35/8/89 - 10.1149/1.3567740
Rights	© The Electrochemical Society, Inc. 2011. All rights reserved. Except as provided under U.S. copyright law, this work may not be reproduced, resold, distributed, or modified without the express permission of The Electrochemical Society (ECS). The archival version of this work was published in Collins, G., Fleming, P., O'Dwyer, C., Morris, M. A., Holmes, J. D. (2011) 'Functionalization of Germanium Nanowires'. ECS Transactions, 35(8), pp. 89-99; doi:10.1149/1.3567740
Download date	2025-07-03 23:22:48
Item downloaded from	https://hdl.handle.net/10468/991



UCC

University College Cork, Ireland
Coláiste na hOllscoile Corcaigh

Functionalization of Germanium Nanowires

G. Collins^{a,b}, P. Fleming^{a,b}, C. O'Dwyer^c, M. A. Morris^{a,b} and J. D. Holmes^{a,b}

^a Department of Chemistry and the Tyndall National Institute, University College Cork, Cork, Ireland.

^b Centre for Research on Adaptive Nanostructures and Nanodevices (CRANN), Trinity College Dublin, Dublin 2, Ireland.

^c Department of Physics and Materials and Surface Science Institute (MSSI), University of Limerick, Limerick, Ireland.

Halogen-termination and organic functionalization of germanium (Ge) nanowires is described. X-ray photoelectron spectroscopy (XPS), X-ray photoemission electron spectroscopy (XPEEM), infrared spectroscopy (IR) and transmission electron spectroscopy (TEM) were used to characterize the modified nanowire surfaces. The stability of alkyl and alkanethiol monolayers formed on Cl, Br and I-terminated surfaces are compared. The direct covalent attachment of aryl ligands onto H-Ge nanowires can be achieved by the decomposition of arenediazonium salts in acetonitrile solutions. The influence of the ring substituent on the thickness and uniformity of the functionalization layer was investigated.

Introduction

Germanium (Ge) offers potential advantages over silicon (Si) for performance gains in high speed electronic devices due to greater free carrier mobility¹⁻². There have been advances in Ge nanowire growth and several groups have already demonstrated the fabrication of single Ge nanowire devices such as field effect transistors (FETs)³⁻⁵ and *p-n* junctions⁶. However, Ge possesses an unstable, non-uniform oxide surface on both bulk and nanowire surfaces which gives rise to a poor Ge/GeO_x interface characterized by a high density of surface states⁷⁻⁸. The negative influence of these surface states on the electrical properties of nanowires has been theoretically and experimentally studied⁹⁻¹². The successful integration of Ge nanowires into many device applications consequently requires effective surface oxide removal and passivation. This paper describes the organic surface functionalization of hydride and halogenated Ge nanowires. Alkylation and thiolation of the halogenated Ge nanowires was carried out using alkyl Grignard reagents and alkanethiols, respectively. The stability of the alkyl and alkanethiol passivation layers produced from the different halogen-terminated surfaces was investigated. The use of arenediazonium salts as precursors for Ge surface modification was also investigated. Reaction of H-terminated Ge surfaces with arenediazonium salts resulted in the covalent attachment of aromatic ligands onto the nanowire surface. The morphology of the functionalized nanowires was characterized by transmission electron microscopy (TEM).

Experimental

Ge Nanowire Synthesis

The Ge nanowires used in this study were synthesized by the thermal decomposition of diphenylgermane (purchased from ABCR, Germany) in the presence of gold-coated silicon substrates in supercritical (sc) toluene. Details of the experimental set-up have been described elsewhere¹³. The reactions were carried out at a temperature and pressure of 400 °C and 24.1 MPa, respectively, yielding nanowires with a mean diameter of 80 nm. The nanowires displayed a predominately <111> growth direction, with <110> and <112> growth directions also present.

Alkyl and Alkanethiol Functionalization

Diethyl ether (Et₂O) was distilled from Na/benzophenone and anhydrous methanol (MeOH) and isopropyl alcohol (IPA) were purchased from Sigma Aldrich. All other reagents were purchased from Sigma Aldrich. All organic functionalization procedures were carried under an inert atmosphere (N₂ filled glovebox, or Ar Schlenk line). Halogen termination of the Ge nanowires was carried out by immersing the nanowires into 10 % aqueous HCl, HBr and 5 % aqueous HI solutions for 10 min. The substrates were washed with deionized water, IPA and dried under N₂. The Ge halogenated nanowires were functionalized with alkyl chains by immersion into a 1 M dodecylmagnesium bromide (DD-MgBr) in Et₂O and heated to 45 °C for 24-72 h. After the reaction the substrates were soaked in anhydrous Et₂O for 5 min and then rinsed with more Et₂O. This soaking/rinsing procedure was repeated 3 times. The nanowires were then rinsed with MeOH and dried under N₂. Ge nanowires were passivated with alkanethiols by immersion into 0.1 M dodecanethiol in anhydrous IPA heated to 60 °C for 2-24 h. Following the passivation procedure the substrates were soaked in IPA for 5 min and rinsed with IPA (× 3). The nanowires were then rinsed with chloroform, MeOH and dried with N₂.

Functionalization of Ge Nanowires using Arenediazonium Salts

The arenediazonium tetrafluoroborate salts were synthesized from the corresponding anilines according to literature procedures¹⁴. Acetonitrile (MeCN) was distilled from calcium hydride onto freshly prepared molecular sieves (3 Å). The native Ge oxide was first removed by immersing the nanowires into 5 % aqueous HF solution for 5 min. The nanowires were then rinsed with deionized water, dried with Ar and transferred into a N₂ glovebox (< 1 ppm O₂). The nanowires were immersed in freshly prepared diazonium salt solutions (1-5 mM) in anhydrous de-oxygenated MeCN. Functionalization reactions were carried out at room temperature in a glove box, or at 50 °C on a Schlenk line under an Ar atmosphere. Reaction times of ranging from 0.5, 2, 12 and 24 h were used. After functionalization the nanowires were immersed in MeCN, soaked for 5 min and then rinsed with more MeCN. The nanowires were then washed with anhydrous MeOH followed by drying under a stream of N₂.

Materials Characterization

Scanning electron microscopy (SEM) images were acquired on a FEI Inspect F, operating at 5 kV accelerating voltage. Transmission electron microscopy (TEM) images were acquired on a Jeol 2100 operating at voltage 200 kV accelerating voltage. X-ray

photoelectron spectroscopy (XPS) analysis was conducted on a VSW Atom tech System with a twin anode X-ray source (Al/Mg).

Results and Discussion

Alkyl and Alkanethiol Functionalized Ge Nanowires

Fig. 1 (a) illustrates an SEM image of Au-seeded Ge nanowires used in this study. The nanowires possess a native oxide, typically 2-5 nm in thickness, as illustrated in the TEM image shown in Fig 1 (b). The Ge $3d$ XPS core level spectra shown in Fig. 1(c) comprises of an elemental Ge peak, which exhibits spin-orbit splitting of 0.585 eV, consistent with that of the Ge $3d_{5/2}$ and Ge $3d_{3/2}$ peaks, located at 28.6 eV and 29.2 eV, respectively¹⁵. In addition to bulk Ge, 4 oxide associated peaks are present at higher binding energies. H- and halogen (Cl, Br, I)-terminated Ge surfaces can be readily prepared by treatment with aqueous halogenic acid solutions. The stability of these passivation layers increases with the increasing size of the passivating species, i.e. in $H < Cl < Br < I$ ¹⁶.

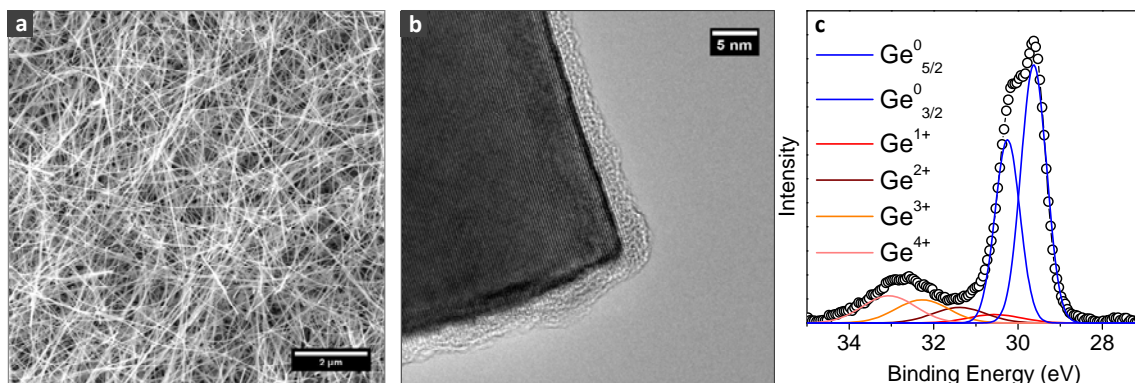


Fig. 1 (a) SEM image of Ge nanowires, (b) TEM image of oxidized Ge nanowire and (c) Ge $3d$ XPS core level spectra for oxidized Ge nanowires.

XPEEM measurements, shown in Fig 2, were used to evaluate the surface coverage of Br and I passivated Ge nanowires. The presence of Br and I species on the nanowire surface was clearly observed in the Br $3d$ and I $4d$ PEEM images and spectra, Fig 2 (a)-(c) and (d)-(f), respectively. The halogen surface coverage can be estimated from the integral intensities of the Ge and halogen XPEEM spectra. The intensities were corrected for spectra that were collected at different photon energies. A detailed description of the XPEEM data analysis is described elsewhere¹⁷⁻¹⁸. The monolayer surface coverage (θ_x) was estimated from equation (1):

$$\theta_x = \frac{I_x / \sigma_x}{(I_x / \sigma_x) + (I_{Ge} / \sigma_{Ge})} \quad (1)$$

Where I_x and I_{Ge} are the integrated intensities of the Ge and halogen species, respectively, and σ_x , σ_{Ge} are the corresponding photoionization cross sections taken from literature values¹⁹. The estimated values for θ_{Br} and θ_I were found to be 1.04 and 0.91, respectively. It must be noted that errors such as non-linear background and

approximations in photoemission cross-sections introduce errors in the surface coverage calculations, estimated to be ± 0.2 .

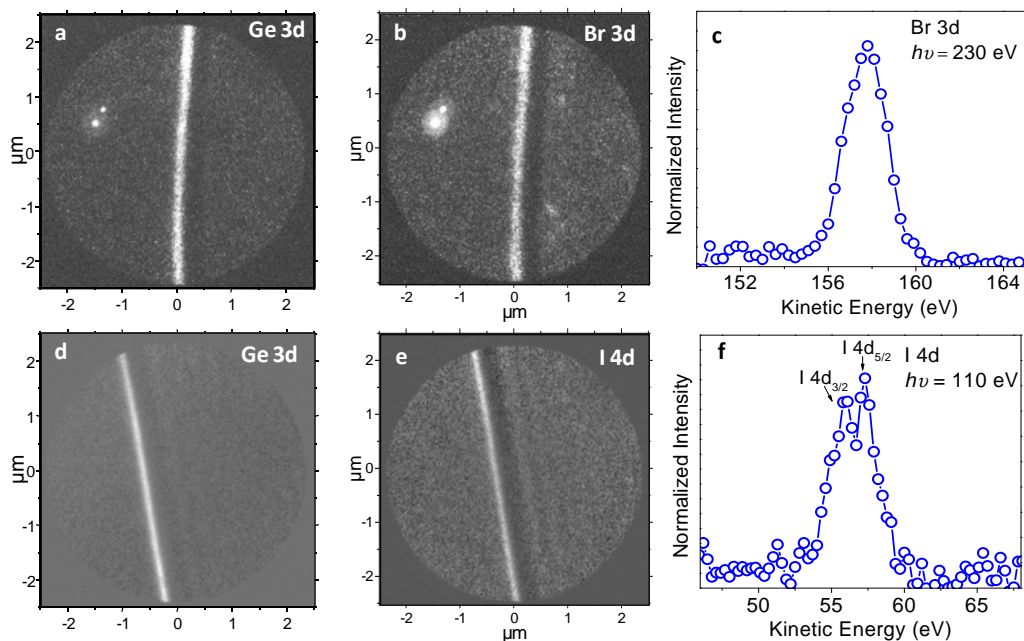


Fig. 2 XPEEM images and spectra of (a-c) Br-terminated nanowires, illustrating the Br $3d$ spectra and (d-f) I-terminated Ge nanowires, illustrating the I $4d$ spectra.

Fig. 3 illustrates XPS spectra of Cl-terminated Ge nanowires as well as alkane and alkanethiol functionalized nanowires, obtained via chlorinated surfaces. After alkylation with DD-MgBr there is an increase in the intensity of the C $1s$ peak relative to the chlorinated nanowires. After reacting the Cl-terminated Ge nanowires with Grignard reagents for 24 h, Cl species are still observed in the XPS survey as shown by the presence of the Cl $2s$ and Cl $2p$ peaks at binding energies of 269 and 200 eV, respectively in the survey spectra can be observed. After 48 h, there was a reduction in the intensity of the Cl $2s$ peak, however the complete removal of Cl species on the alkylated surfaces was not achieved. The high resolution Cl $2s$ spectrum shown in Fig. 3(b), taken after a reaction time of 72 h, indicates that some Cl atoms still remain on the nanowire surface.

In comparison to alkylation, thiolation reactions on chlorinated Ge surfaces showed no Cl species in the XPS analysis after a reaction time of 4 h, as shown in the high resolution Cl $2s$ spectrum in Fig. 3(c). Fig. 3(d) displays the high resolution S $2p$ XPS core level spectra of the thiolated nanowires prepared from Cl, Br and I-terminated surfaces. The reaction proceeded on all of the halogenated surfaces and the S $2p$ peak, which is centered at 162.7 eV, is in good agreement of with binding energies reported for thiolated monolayers²⁰⁻²².

The absence of halogen species in the XPS survey spectra, after thiol functionalization indicates that alkanethiols are more effective in replacing surface halogen species compared to alkyl Grignard reagents. After ~ 72 h immersion in the Grignard solution there is negligible change in the intensity of the Ge:halogen XPS peaks, indicating that further reaction with the remaining halogen species is unfavorable. It is well known that the structure of alkyl Grignard reagents in solution is described by the Schlenk

equilibrium which involves the co-ordination of solvent molecules to the Mg atom²³. Furthermore, ethereal solutions of Grignard reagents in a concentration range of 0.5-1 M exist as dimeric complexes²⁴. Increased steric effects experienced by Grignard reagents due to solvent co-ordination may also hinder the ability to access the halogenated species on the nanowire surface, consequently resulting in unreacted residual halogen species detected by XPS analysis.

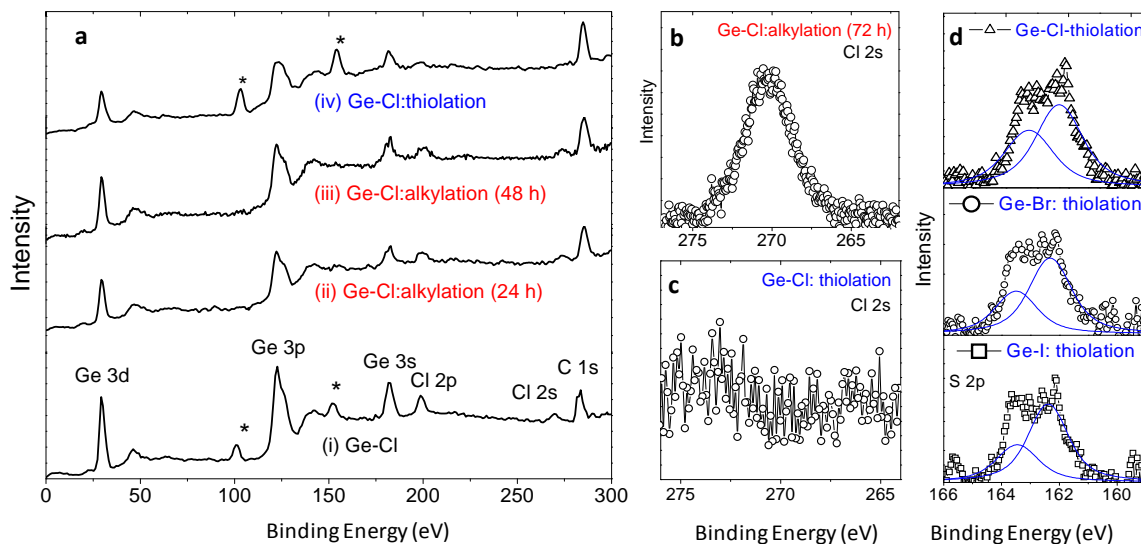


Fig. 3 (a) XPS survey scans of Cl-terminated Ge nanowires and alkylation and thiolation functionalization via chlorinated surfaces, (b) Cl 2s core-level spectrum showing the presence of Cl after an alkylation reaction time of 72 h, (c) Cl 2s core-level spectrum after thiol functionalization showing no Cl species present, (d) S 2p core-level spectra of Ge nanowires thiolated from Cl, Br and I-terminated surfaces. The asterisks indicate signals from the Si wafer.

Table 1 displays the aliphatic IR stretching frequencies of alkyl and alkanethiol functionalized Ge nanowires. The C-H symmetric and asymmetric stretches occur at $\sim 2850\text{ cm}^{-1}$ and 2920 cm^{-1} , respectively. These peak positions are in good agreement with IR absorbance frequencies reported by Kosuri *et al.*²⁵ for alkanethiol functionalized bulk Ge surfaces. The peak positions of the C-H stretching modes occur at lower frequencies relative to isotropic liquid DDT, indicating a degree of crystalline order is present in the alkanethiol passivation layer²⁶⁻²⁸. However, the asymmetric CH_2 stretching mode of highly crystalline hydrocarbons typically appears at 2918 cm^{-1} ²⁶, suggesting that some disorder is present in the alkyl and thiol functionalization layers. The vibrational modes for alkylation via I-terminated surfaces exhibit the highest absorption frequencies ($\nu_{\text{as}}\text{CH}_2$: 2925 cm^{-1} , $\nu_{\text{a}}\text{CH}_2$ 2851 cm^{-1} , $\nu_{\text{a}}\text{CH}_3$: 2960 cm^{-1}) indicating the most disordered passivation layer was achieved via an iodination/alkylation route. The presence of unreacted halogen species or defects at the nanowire surface would be expected to disrupt the ordering and assembly of the passivating ligands.

TABLE 1. IR stretching frequencies for alkyl and alkanethiol functionalized Ge nanowires

Halogen	ν_s (CH ₂)	ν_{as} (CH ₂)	ν_{as} (CH ₃)
Alkylation IR Frequencies			
(-Cl)	2852 cm ⁻¹	2922 cm ⁻¹	2956 cm ⁻¹
(-Br)	2849 cm ⁻¹	2920 cm ⁻¹	2953 cm ⁻¹
(-I)	2851 cm ⁻¹	2925 cm ⁻¹	2960 cm ⁻¹
Thiolation IR Frequencies			
(-Cl)	2850 cm ⁻¹	2920 cm ⁻¹	2956 cm ⁻¹
(-Br)	2850 cm ⁻¹	2920 cm ⁻¹	2955 cm ⁻¹
(-I)	2852 cm ⁻¹	2921 cm ⁻¹	2956 cm ⁻¹

Stability of Alkyl and Alkanethiol Passivation Layers

The degree of re-oxidation of the Ge surface provides insight into the quality of the passivation monolayers attained from the halogenated surfaces. Fig. 4(a) and (b) illustrate the XPS Ge 3*d* peaks for Cl/Br/I surfaces functionalized with alkyl and alkanethiols, respectively, after one week exposure to ambient conditions. Overall, Ge nanowires functionalized by alkyl Grignard reagents display a higher degree of re-oxidation compared to alkanethiol passivated surfaces as indicated by the greater oxide component in the Ge 3*d* spectra. A comparison of the spectra within Fig. 4(a) shows that alkyl passivation via chlorinated surfaces exhibit the most oxidation, while passivation via iodinated surfaces shows the least. The opposite trend is observed for alkanethiol passivation, with Ge nanowires thiolated from Cl and Br-terminated surfaces showing no oxidation after ambient exposure for 1 week, while thiolation via iodinated surfaces do exhibit some re-oxidation. The oxide shifted peak in the Ge 3*d* XPS core level spectrum is small, indicating only minor oxidation of the surface.

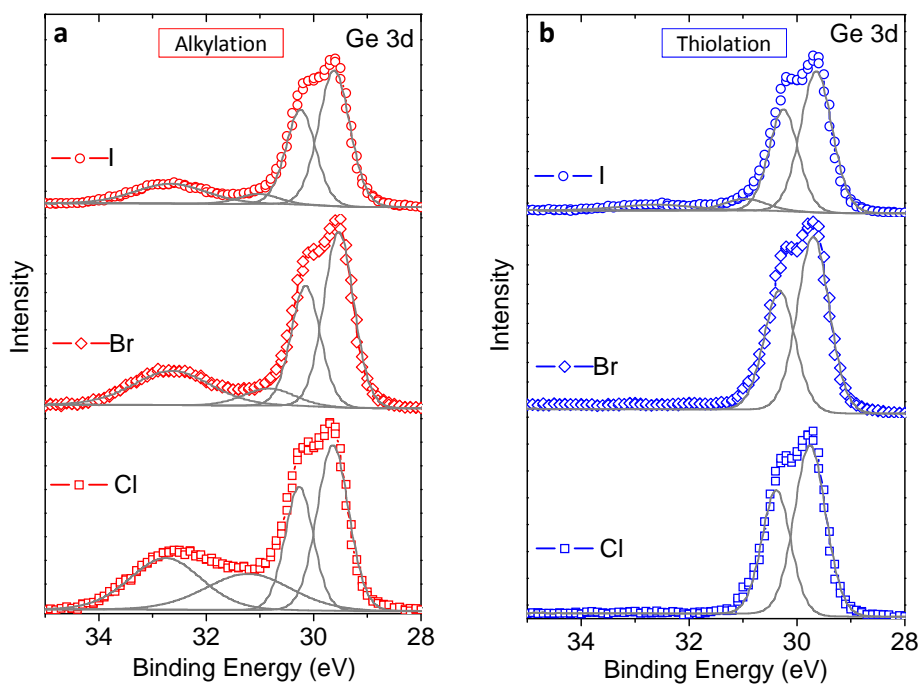


Fig. 4 XPS spectra of (a) dodecyl and (b) dodecanethiol-functionalized Ge nanowires from Cl, Br and I-terminated surfaces after 1 week of ambient exposure.

Functionalization using Arenediazonium Salts

The use of arenediazonium salts as precursors for the surface functionalization of Ge was investigated. Fig. 5(a) shows the N $1s$ core level spectrum of Ge nanowires functionalized using nitrophenyldiazonium tetrafluoroborate (NO₂Ph-BD). The peak located at a binding energy of 405.9 eV is characteristic of the NO₂ group, while the second peak located at a lower binding energy of 399 eV corresponds to a reduced form of nitrogen. Several groups have attributed the latter peak to the reduction of the NO₂ group to amines (-NH₂) under the XPS beam²⁹⁻³¹, while others have associated the peak at ~400 eV to the presence of azo (N=N) or azoxy (N=N-O) species that are incorporated into the functionalization layer during the reaction³²⁻³⁴. Importantly, the absence of a peak associated with the diazonium group (N≡N⁺) at ~402 eV³⁵, suggests that the salt has reacted with the Ge surface. Further evidence for covalent attachment of the aromatic ligands is provided by the IR spectra, as illustrated in Fig. 5 (b), which compares the bulk arenediazonium salts and functionalized Ge nanowires. The Ge nanowire spectra display several structural features associated with the passivating ligands; the symmetric (ν_s) and asymmetric (ν_{as}) NO₂ stretches are observed at 1346 cm⁻¹ and 1522 cm⁻¹, respectively³⁶. The C=C stretching vibration was also observed at 1597 cm⁻¹. Notably, there is a disappearance of the vibrational band at 2250 cm⁻¹, characteristic of the N₂⁺ group and the absence of the strong broad absorption peak for BF₄⁻, located at ~1050 cm⁻¹²⁹. The absence of these features is consistent with the XPS analysis and suggests the diazonium salt moiety (N₂⁺BF₄⁻) is no longer associated with the ligands.

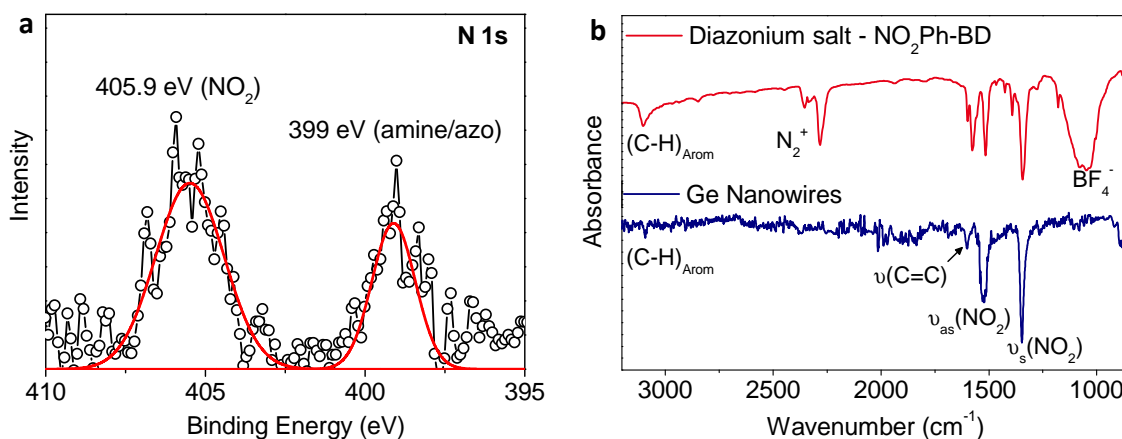


Fig 5. (a) N $1s$ XPS core level spectrum of H-terminated Ge nanowires functionalized with NO₂Ph-BD. (b) ATR-IR spectra of NO₂Ph-BD salt and functionalized Ge nanowires.

Nanowires functionalized by immersion into NO₂Ph-BD solutions for 2 h and 12 h are compared in Fig. 6 (a) and (b), respectively. A reaction time of 2 h yielded a thin (1.5 – 2 nm) homogenous organic layer on the nanowire surface. After a 12 h reaction time, the thickness of the organic film increased to ~4 nm, accompanied by a slight decrease in uniformity relative to the thinner functionalization layer. TEM analysis suggested that the presence of aryl multilayers, which form as a result of an aryl radical attaching to an already covalently bound ligand, as illustrated by the schematic in Fig. 6(c).

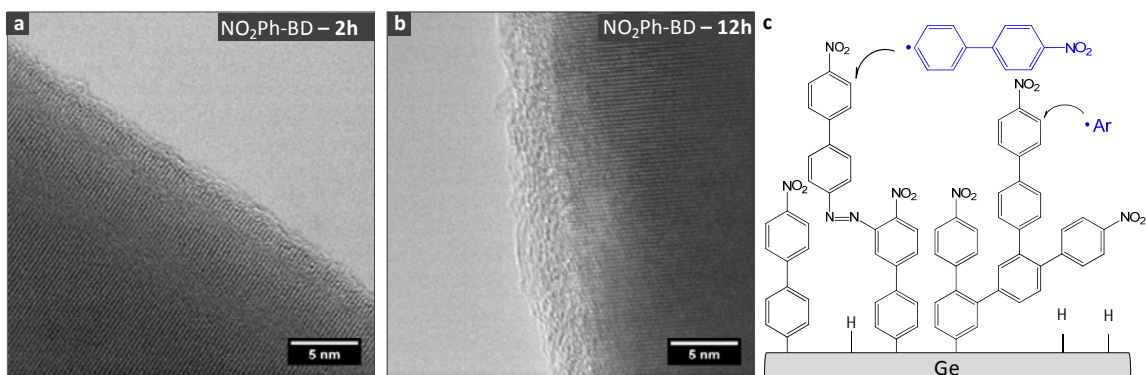


Fig. 6 TEM image of Ge nanowire functionalized with NO₂Ph-BD using a reaction time of (a) 2 h and (b) 12 h. (c) Schematic illustrating the radical mechanism for multilayer formation.

The addition of aryl radicals to form multilayers proceeds preferentially via attack at the 3- and 5- ring positions (numbered relative to the diazonium group). Fig. 7 (a)-(c) display a 40 nm and an 11 nm Ge nanowire modified with 3, 4, 5-trifluorobenzenediazonium (F₃-BD). The influence of ring substituents on multilayer formation is apparent from the thickness of the functionalization layer; after a 12 h reaction time the organic layer remained thin (~ 1-2 nm) and did not undergo multilayer formation as observed with NO₂Ph-BD. In F₃-BD the 3-, 4- and 5- ring positions contain F substituents and therefore blocked towards further attack from aryl radicals. Side reactions with F₃-BD can only proceed via radical attack on the 2- and 6- positions, which is disfavoured by steric constraints from the nanowire surface, as illustrated by the schematic shown in Fig 7. Fig 7 (d) shows the IR spectra of F₃-DB modified nanowires to confirm the presence of the organic functional layers. The absence of vibrational bands attributed to the N₂⁺ and BF₄⁻ groups in the functionalized Ge nanowires suggest a reaction with the surface. The nanowire spectrum displays the presence of the =C-F absorption at 1242 cm⁻¹, typical of aromatic fluorocarbons³⁷, as well as the presence of the C=C stretching vibration at 1518 cm⁻¹. Due to the high electronegativity of F substituents, the intensity of the C-H in-plane bending vibration is greatly enhanced and this can be seen at 1020 cm⁻¹³⁸. The results here illustrate the potential of arenediazonium salts as precursors for the functionalization of Ge nanowires, which may allow for the controlled growth of multilayer thin films or organic monolayers on the nanowire surface.

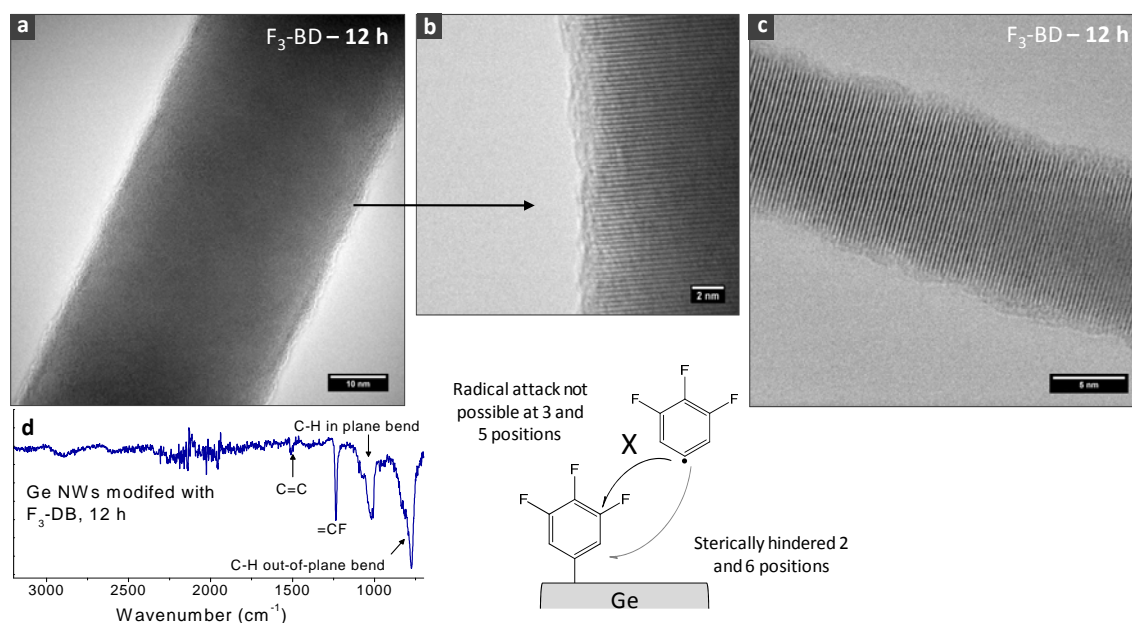


Fig. 7 (a)-(b) 40 nm and (c) 11 nm Ge nanowire functionalized with F_3 -BD, scale bars 10, 2 and 5 nm, respectively. (d) ATR-IR spectra of F_3 -BD modified Ge nanowires.

Conclusions

Organic functionalization of hydride and halogenated (Cl, Br, I) nanowires was investigated. Attachment of dodecyl chains via Grignard reagents did not result in complete removal of the surface halogens, even after long reaction times. Conversely, after thiolation of the nanowire surfaces no halogen species were detected by XPS. Incomplete surface functionalization via Grignard reagents was also reflected in stability studies of the alkane and alkanethiol functionalized nanowires. After exposure to ambient conditions for 1 week the alkylated nanowires showed a greater degree of re-oxidation relative to thiolated nanowire surfaces. On the other hand, alkanethiol passivation layers showed excellent ambient stability; functionalization from Cl and Br surfaces showed no re-oxidation of the surface after 1 week, while those formed from iodated surfaces only exhibited minor oxidation.

Functionalization of H-terminated Ge nanowire surfaces with aromatic ligands is possible through the decomposition of arenediazonium salts in MeCN solutions. XPS and ATIR analysis clearly identifies the spectral signatures of the functionalization ligands on the Ge nanowires while also indicating the loss of the N_2^+ and BF_4^- functional groups. The nature of the ring substituents was found to influence the structure of the organic functionalization layer obtained on the Ge nanowires. For mono-substituted arenediazonium salts the thickness of the organic layer increases with reaction time due to the formation of aryl multilayers. Highly substituted aromatic rings however, resulted in thin functionalization layers as multilayer formation is hindered.

Acknowledgments

This work was financially supported by the Irish Research Council for Science and Engineering Technology (IRCSET) and Science Foundation Ireland (Grant 08/CE/I1432). Part of this work was conducted under the framework of the INSPIRE programme, funded by the Irish Government's Programme for Research in Third Level Institutions, Cycle 4, National Development Plan 2007-201. We would also like to thank Michael Schmidt in the Electron Microscopy and Analysis Facility (EMAF) at the Tyndall National Institute, Ireland, for help with HRTEM imaging. We would like to thank the researchers at the Trieste Synchrotron Facility, Italy for their assistance in the XPEEM measurements.

References

1. B. Yu, X. H. Sun, G. A. Calebotta, G. R. Dholakia and M. Meyyappan, *J. Cluster Sci.*, **17** (4), 579, (2006).
2. P. R. Bandaru and P. Pichanusakorn, *Semicond. Sci. Technol.*, **25** 024003, (2010).
3. A. B. Greytak, L. J. Lauhon, M. S. Gudiksen and C. M. Lieber, *Appl. Phys. Lett.*, **84** (21), 4176, (2004).
4. K. C. Saraswat, C. O. Chui, T. Krishnamohan, A. Nayfeh and P. McIntyre, *Microelectron. Eng.*, **80** 15, (2005).
5. D. W. Wang, Y. L. Chang, Q. Wang, J. Cao, D. B. Farmer, R. G. Gordon and H. J. Dai, *J. Am. Chem. Soc.*, **126** (37), 11602, (2004).
6. E. Tutuc, J. Appenzeller, M. C. Reuter and S. Guha, *Nano Lett.*, **6** (9), 2070, (2006).
7. V. V. Afanas'ev, Y. G. Fedorenko and A. Stesmans, *Appl. Phys. Lett.*, **87** (3), (2005).
8. M. Houssa, E. Chagarov and A. Kummel, *MRS Bull.*, **34** 504, (2009).
9. T. Hanrath and B. A. Korgel, *J. Phys. Chem. B*, **109** (12), 5518, (2005).
10. D. Medaboina, V. Gade, S. K. R. Patil and S. V. Khare, *Phys. Rev. B*, **76** 205327, (2007).
11. L. C. L. Y. Voon, Y. Zhang, B. Lassen, M. Willatzen, Q. Xiong and P. C. Eklund, *J. Nanosci. and Nanotechnol.*, **8** 1, (2008).
12. R. P. Prasankumar, S. Choi, S. A. Trugman, S. T. Picraux and A. J. Taylor, *Nano Lett.*, **8** (6), 1619, (2008).
13. J. Chlistunoff, K. J. Ziegler, L. Lasdon and K. P. Johnston, *J. Phys. Chem. A*, **103** 1678, (1999).
14. M. P. Stewart, F. Maya, D. V. Kosynkin, S. M. Dirk, J. J. Stapleton, C. L. McGuinness, D. L. Allara and J. M. Tour, *J. Am. Chem. Soc.*, **126** (370), (2004).
15. D. Schmeisser, R. D. Schnell, A. Bogen, F. J. Himpsel and D. Rieger, *Surf. Sci.*, **172** 455, (1986).
16. H. Jagannathan, J. Kim, M. Deal, M. Kelly and Y. Nishi, *ECS Trans.*, **3** (7), 1175, (2006).
17. F. Ratto, A. Locatelli, S. Fontana, S. Kharrazi, S. Ashtaputre, S. K. Kulkarni, S. Heun and F. Rosei, *Small*, **2** (3), 401, (2006).
18. F. Ratto, F. Rosei, A. Locatelli, S. Cherifi, S. Fontana and S. Heun, *J. Appl. Phys.*, **97** 043516, (2005).
19. J. J. Yeh and I. Lindau, *At. Nucl. Data Tables*, **32** (1), 1, (1985).

20. Y. Jun, X. Y. Zhu and J. W. P. Hsu, *Langmuir*, **22** (8), 3627, (2006).
21. R. Desikan, S. Armel, H. M. Meyer and T. Thundat, *Nanotechnology*, **18** (42), (2007).
22. P. Ardalan, Y. Sun, P. Pianetta, C. B. Musgrave and S. F. Bent, *Langmuir*, **26** (11), 8419, (2010).
23. G. S. Silverman and P. E. Rakita, *Handbook of Grignard Reagents*, Marcell Dekker Inc., (1996).
24. E. C. Asbey and M. Smith, *J. Am. Chem. Soc.*, **86** (20), 4363, (1964).
25. M. R. Kosuri, R. Cone, Q. M. Li, S. M. Han, B. C. Bunker and T. M. Mayer, *Langmuir*, **20** (3), 835, (2004).
26. F. Bensebaa, R. Voicu, L. Huron, T. H. Ellis and E. Kruus, *Langmuir*, **13** 5335, (1997).
27. M. R. Linford, P. Fenter, P. M. Eisenberger and C. E. D. Chidsey, *J. Am. Chem. Soc.*, **117** 3145, (1995).
28. V. C. Holmberg and B. A. Korgel, *Chem. Mat.*, **22** (12), 3698, (2010).
29. A. Adenier, E. Cabet-Deliry, A. Chausse, S. Griveau, F. Mercier, J. Pinson and C. Vautrin-UI, *Chem. Mater.*, **17** (3), 491, (2005).
30. P. Mendes, M. Belloni, M. Ashworth, C. Hardy, K. Nikitin, D. Fitzmaurice, K. Critchley, S. Evans and J. Preece, *ChemPhysChem*, **4** (8), 884, (2003).
31. S. Q. Lud, M. Steenackers, R. Jordan, P. Bruno, D. M. Gruen, P. Feulner, J. A. Garrido and M. Stutzmann, *J. Am. Chem. Soc.*, **128** 16884, (2006).
32. S. S. C. Yu, E. S. Q. Tan, R. T. Jane and A. J. Downard, *Langmuir*, **23** (22), 11074, (2007).
33. D. M. Shewchuk and M. T. McDermott, *Langmuir*, **25** (8), 4556, (2009).
34. P. Doppelt, G. Hallais, J. Pinson, F. Podvorica and S. Verneyre, *Chem. Mater.*, **19** (18), 4570, (2007).
35. S. Szunerits and R. Boukherroub, *J. Solid State Electrochem.*, **12** 1205, (2008).
36. B. Smith, *Infrared Spectral Interpretation: A systematic Approach*. (CRC Press, Boca Raton, Florida, 1999).
37. L. A. Wall, R. E. Donadio and W. J. Pummer, *J. Am. Chem. Soc.*, **82** (18), 4846, (1960).
38. J. Coates, in *Encyclopedia of Analytical Chemistry*, edited by R. A. Meyers (John Wiley & Sons Ltd., Chichester, 2000), pp. 10815.